Probing hyperfine interactions in 53Cr(III) doped Al2O3 by spectral hole-burning in low magnetic fields

Riesen, Hans; Szabo, Alex

Publisher's version / Version de l'éditeur:
https://doi.org/10.1016/j.phpro.2010.01.224
Physics Procedia, 3, 4, pp. 1577-1582, 2010-02-28

Available online at www.sciencedirect.com
ScienceDirect
Physics Procedia 3 (2010) 1577–1582
Physics Procedia
www.elsevier.com/locate/procedia

Proceedings of HBSM 2009

Probing hyperfine interactions in $^{53}Cr(III)$ doped Al_2O_3 by spectral hole-burning in low magnetic fields.

Hans Riesen[a]* and Alex Szabo

[a]*School of Physical, Environmental and Mathematical Sciences, The University of New South Wales, ADFA, Northcott Drive, Canberra, ACT 2600, Australia*

[b]*Institute for Microstructural Sciences, National Research Council of Canada, 1200 Montreal Road, Ottawa, Ontario K1A 0R6, Canada*
Received 10 November 2009; revised 20 November 2009; accepted 20 November 2009

Abstract

We report transient spectral hole-burning experiments conducted in the $R_1(\pm 1/2)$ line of 53-chromium(III) doped Al_2O_3 in zero field and low magnetic fields B||c at 3 K. These facile experiments enable, in principle, the simultaneous determination of the hyperfine coupling parameters for both the $^4A_2$ ground state and the $\bar{E}(^2E)$ excited state, and in both directions to the crystal *c*-axis. In order to determine these parameters we have applied a global fit by simulated spectra to the experimental data and good agreement between calculated and measured hole-burning patterns is achieved. The relevant resulting parameters for the $\bar{E}(^2E)$ excited state are A||=18±4 MHz and A⊥=40±4 MHz.

Keywords: transient spectral hole-burning; ruby; 53-chromium(III); hyperfine interaction

1. Introduction

Ruby (Al_2O_3/Cr(III)) has played an important role as an archetypal system for the spectroscopy of impurity ions in insulators over the last 140 years. Major milestones in this field include Becquerel's report of the so-called R-lines ($^4A_2 \leftarrow ^2E$ transitions) in 1870 [1]; Sugano and Tanabe's detailed paper on ligand field theory in 1958 [2]; Maiman demonstration of the first laser action in 1960 [3]; Kurnitt, Abella and Hartman report on the first observation of photon echo experiment in the solid state in 1964 [4]; Szabo's first fluorescence line narrowing and first transient spectral hole-burning experiment in the solid state in 1971 and 1975, respectively, [5,6] which was followed by detailed investigations by a range of hole-burning experiments [7-15]; Macfarlane et al.'s photon-echoes in the superhyperfine limit in 1991 [16]; and Riesen et al.'s observation of side-hole to anti-hole conversion caused by population storage in the ground state in 2007 [17]. The stable isotopes ^{50}Cr, ^{52}Cr, ^{53}Cr and ^{54}Cr occur

*Corresponding author. Tel.: +61-2-6268-8679; fax: +61-2-6268-8017.
E-mail address: h.riesen@adfa.edu.au

doi:10.1016/j.phpro.2010.01.224

with natural abundancies of about 4.3, 83.8, 9.6 and 2.3 %, respectively. The ^{53}Cr is the only stable isotope with a nuclear spin (I=3/2). Hence in standard ruby samples the ^{52}Cr(III) ion dominates most optical spectroscopy. Nevertheless, the ^{53}Cr(III) ion can be observed in laser spectroscopy and the R_1-line is blueshifted by 3.6 GHz in comparison with the ^{52}Cr(III) ion [13]. Thus it is not surprising that the ^{52}Cr isotope has received most attention in Al_2O_3/Cr(III), and little work has been conducted on the I=3/2 ^{53}Cr(III) isotope in the Al_2O_3 host. In some very early work, Geschwind et al. [18] investigated spin-lattice relaxation rates and the hyperfine structure in the $\overline{E}$ (^{2}E) state of a Al_2O_3 sample doped with Cr enriched to 92 % ^{53}Cr, by optical-radiofrequency double resonance experiments and they concluded that the hyperfine coupling constant A|| is <6 MHz in the $\overline{E}$ (^{2}E) level. Geschwind et al. [18] could not estimate a value for A⊥ as their work was conducted in a magnetic field parallel the c axis of about B||=0.7 T. Fig. 1 shows data adapted from this early work.

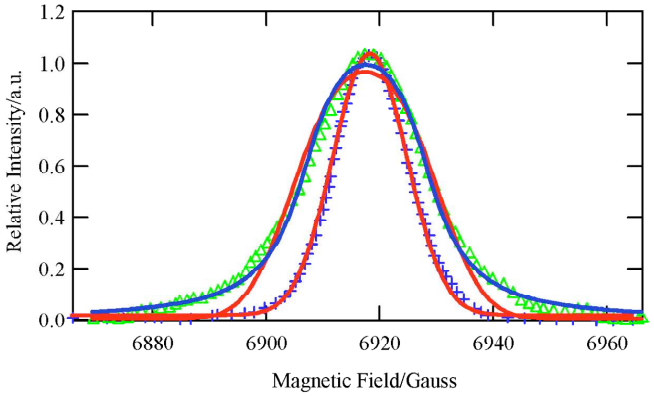

Fig. 1. Optically detected EPR signal in the $\overline{E}$(^{2}E) state of Al_2O_3/^{52}Cr(III) (blue crosses) and Al_2O_3/ ^{53}Cr(III) (green triangles) with fit lines consisting of one and four Gaussians, respectively, (red lines) and the sum of four Lorentzians (blue line). The microwave frequency was at the fixed frequency of 23672 MHz for this experiment. The data has been adapted from reference [18].

An analysis of the data in Fig. 1 yields a FWHM of 13 Gauss (=44 MHz) for the Al_2O_3/^{52}Cr data; fitting the sum of four Lorentzians or four Gaussians with this value for the FWHM of the linewidth to the Al_2O_3/^{53}Cr data, estimates of A||=17 and 22 MHz, respectively, result for the $\overline{E}$ (^{2}E) state.

Szabo *et al* [13] reported nuclear spin-echo decay of the ^{27}Al frozen core, surrounding ^{53}Cr (in a ruby with 9.6% natural abundance), observed by Raman heterodyne detection. These experiments allowed the determination of Cr-Cr spin-flip times and it was concluded that indirect Cr-Cr spin-flipping is the major contributor to optical dephasing for ruby with Cr concentrations up to 0.05 wt% Cr_2O_3.

Some recent work reported photon-echoes in Al_2O_3/^{53}Cr but no comprehensive data analysis was presented [19].

The present paper is a short report on our attempts to deduce the values of the hyperfine coupling constants in the $\overline{E}$ (^{2}E) excited state by facile diode laser based transient spectral hole-burning in low magnetic fields B||c.

2. Experiment

Boules of Verneuil-grown (flame fusion) samples Al_2O_3 doped with 10 ppm Cr enriched to 95 % ^{53}Cr were custom grown by Hrand Djevahirdjian SA, Monthey, Switzerland. The crystals were cut and polished parallel and perpendicular to the crystal c-axis with diamond-impregnated tools. For the transient hole-burning experiments, a crystal with a thickness of ~7 mm was used with the magnetic field (provided by external Helmholtz coils <16 mT) parallel the c-axis in transverse geometry.

Spectral hole-burning experiments were conducted with an external cavity diode laser (Toptica DL100 with DC110 controller). To minimize effects of cross-relaxation and spin-lattice relaxation, pulsed (1 Hz repetition rate) hole-

burning experiments were conducted by passing the laser through a mechanical shutter (Vincent Uniblitz VS14S1T0) that was controlled by a Uniblitz VMM-T1 driver/timer. The shutter was opened for 8 ms and the laser frequency was kept constant during the initial phase of the pulse (2 ms) and then swept over ~2 GHz within 2 ms by applying a triangular voltage ramp (Stanford Research Instruments synthesized function generator model DS345) to the piezoelectric element of the DL100. The laser was focused onto the sample after attenuation by polarizing films and neutral density filters with OD=1 to 3. The effective power level at the sample was less than 50 μW (average power density <50 mW/cm^2). The samples were cooled by a Janis/Sumitomo SHI-4.5 closed-cycle refrigerator. The crystals were embedded with cry-con grease on the cold finger of the cryostat.

3. Results and Discussion

Fig. 2 shows the Zeeman pattern observed in σ-polarized transient hole-burning experiments in the $R_1(\pm 1/2)$ line of the ^{52}Cr(III) isotope in a 20 ppm standard ruby sample in low magnetic fields B||c. Please note the relatively small change in optical density due to the very low chromium concentration and the fact that only shallow holes were burnt. The experimental data is in excellent agreement with the calculated patterns; in these simulations fast Cr-Cr electron spin-spin cross-relaxation in the $^4A_2$ ground state between resonant and non-resonant ions has been assumed [17]. The Zeeman effect with B||c in $Al_2O_3/^{52}Cr$ is well described by the spin-Hamiltonians given in Eqs. (1) and (2). Note that S_z' refers to an effective spin which is +1/2 and -1/2 for the lower (u_+,-1/2) and upper (u_-,+1/2) Zeeman component of $\overline{E}$ (^{2}E) and consequently the *g*-factor of this level is negative.

$$\hat{H}(^4A_2) = g_{||}\mu_B B_{||} S_z + D\left[S_z^2 - \frac{1}{3}S(S+1)\right] \quad (1)$$

$$\hat{H}(^2E) = g_{||}\mu_B B_{||} S_z' \quad (2)$$

In Eqs. (1) and (2), μ_B is the Bohr magneton (13996 MHz/T), B|| is the magnetic field flux (in T) and *D* is the zero field splitting parameter for the $^4A_2$ ground state (2|D|=11447 MHz). The data confirms a factor of $g^{ex}||$=-2.44 for the $\overline{E}$ (^{2}E) state in agreement with early results (e.g. see Ref. [18]). The schematic in Fig. 2 rationalizes the three hole pattern observed in a magnetic field B||c.

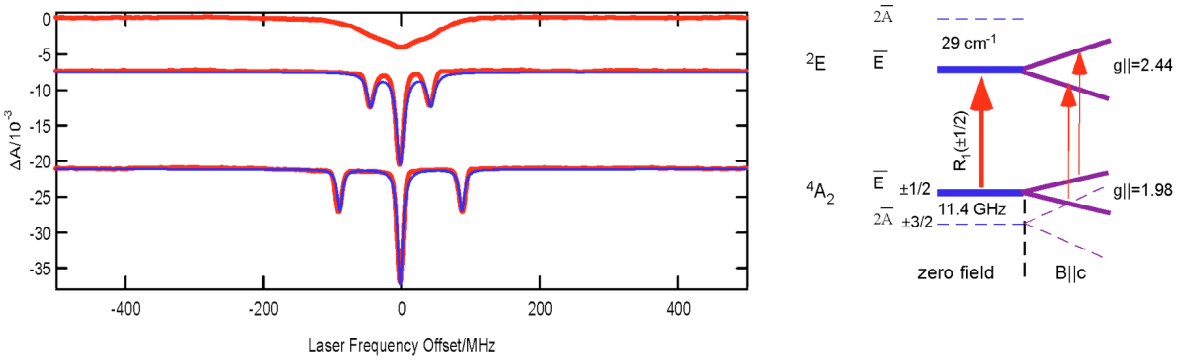

Fig. 2. Zeeman effect in the $R_1(\pm 1/2)$ line in 20 ppm $Al_2O_3/^{53}Cr$ at 3 K as observed in σ-polarized transient spectral hole-burning experiments in low magnetic fields. The red and blue line is observed and calculated, respectively. The schematic on the right hand side shows the transitions that lead to the pattern with sideholes at $\pm\mu_B B||(g^{ex}||-g^{gs}||)$. The magnetic field flux B||c for the traces from top to bottom was 0, 7.28 and 14.9 mT. The hole width in the 7 and 14 mT fields is given by the jitter limited 7.9 MHz linewidth of the laser.

For the ^{53}Cr enriched system the pattern is more complicated since the electronic system and the nuclear spin I=3/2 are coupled. Following spin-Hamiltonians adequately describe the ^{2}E and ^{4}A$_2$ state in a magnetic field B||c.

$$\hat{H}(^4A_2) = g_{\|}\mu_B B_{\|} S_z + D[S_z^2 - \tfrac{1}{3}S(S+1)] + A_{\|} S_z I_z + \tfrac{1}{2}A_{\perp}[S_+ I_- + S_- I_+] - g_I \beta_N B_{\|} I_z + Q'[I_z^2 - \tfrac{1}{3}I(I+1)] \quad (3)$$

$$\hat{H}(^2E) = g_{\|}\mu_B B_{\|} S_z' + A_{\|} S_z' I_z + \tfrac{1}{2}A_{\perp}[S_+ I_- + S_- I_+] - g_I \beta_N B_{\|} I_z + Q'[I_z^2 - \tfrac{1}{3}I(I+1)] \quad (4)$$

In Eqs. (3) and (4), A|| and A⊥ are the hyperfine coupling constants parallel and perpendicular to the *c* axis, respectively, g_I is the nuclear *g*-factor, β_N is the nuclear Bohr magneton and Q' is the nuclear quadrupole interaction constant. Fig. 3 displays data of σ-polarized transient spectral hole-burning spectra in the $R_1(\pm 1/2)$ line of the $Al_2O_3/^{53}Cr$ system at 3 K and in low magnetic fields B||c <7.4 mT in comparison with simulated spectra (again note the low change in optical density due to the low chromium concentration, 10 ppm, and the shallow hole depth).

A Matlab® based code was applied globally to the data illustrated in Fig. 3 in order to extract the hyperfine coupling constants of the $\overline{E}(^2E)$ excited state. This analysis is, to a certain extent, difficult because of the relatively broad hole width observed in the $Al_2O_3/^{53}Cr$ system. For example, in contrast to the $Al_2O_3/^{52}Cr$ system (see Fig. 2) the resonant hole is not narrowed to less than 1 MHz at 7 mT. As a result the multidimensional fit surface has a number of relatively shallow minima. Nevertheless, fit attempts resulted in statistically significant values for A||($\overline{E}(^2E)$) and A⊥($\overline{E}(^2E)$). Some parameters for the calculation of eigenvalues and eigenvectors based on the spin-Hamiltonians of Eqs. (3) and (4) are well established. They include the $^4A_2$ ground state parameters D=-5723.5 MHz, g||=1.983, A⊥($^4A_2$)≈A||($^4A_2$)=50.4 MHz [20], Q'=-0.85 MHz and the $\overline{E}(^2E)$ excited state parameter g||=-2.44. Initial estimates for the parameters A|| and A⊥ were used to evaluate the eigenvalues and eigenvectors of the secular determinant that results from Eq. (4). The approximation was then made that spin relaxation between levels in the excited and ground states is not restricted by some spin selection rules i.e. the same relaxation rate is assumed between different levels of the ground or the excited state. Moreover, it was assumed that for the optical transitions the selection rule ΔI_z=0 is strictly obeyed. For the scaling of the spectra, a parameter, that described the product of the total burn fluence and the transition dipole strength, was used. Resulting transitions between the 16 ($^4A_2$) and 8 ($\overline{E}(^2E)$) eigenstates were then calculated by using the matrix elements of the electric dipole operator, as given in Table 1, and a standard matrix transformation procedure. The accumulated pattern of transitions at discrete frequencies was then convoluted with a Lorentzian with a line width given as an empirical parameter for a particular magnetic field strength. The calculation was iterated until best least-squares agreement between experimental data and the calculated hole-burning spectrum was achieved. This procedure yielded the values A||($\overline{E}(^2E)$) =40±4 MHz, A⊥($\overline{E}(^2E)$)=18±4 MHz and thermalization of 60 % and 20 % for the $\overline{E}(^2E)$ excited and $^4A_2$ ground states, respectively. As is illustrated in Fig. 3 the simulated spectra are in good agreement with the experimental data. The 60% thermalization in the excited state at 3 K is commensurate with the spin-lattice relaxation measurements of Geschwind *et al* [18]. The lesser 20% thermalization is due to the fact that cross-relaxation is harder to achieve in $Al_2O_3/^{53}Cr(III)$ than in $Al_2O_3/^{52}Cr(III)$ because of the larger number (4x more) of levels in the former system.

Table 1. Matrix elements of the electric dipole operator, based on the odd-parity crystal field and spin-orbit interaction, between between the $^4A_2$ ground state and the ^{2}E excited state in ruby [21].

	$^4A_2\,\frac{3}{2}$	$^4A_2\,\frac{1}{2}$	$^4A_2\,-\frac{1}{2}$	$^4A_2\,-\frac{3}{2}$
$^2E\,\frac{1}{2}\,u_+$	$-\pi_\alpha/\sqrt{2}$	$-\sigma_{+\alpha}/\sqrt{3}$	$\sigma_{-\alpha}/\sqrt{6}$	0
$^2E\,-\frac{1}{2}\,u_+$	0	$-\pi_\alpha/\sqrt{6}$	$-\sigma_{+\alpha}/\sqrt{3}$	$\sigma_{-\alpha}/\sqrt{2}$
$^2E\,\frac{1}{2}\,u-$	$\sigma_{+\alpha}/\sqrt{2}$	$\sigma_{-\alpha}/\sqrt{3}$	$\pi_\alpha/\sqrt{6}$	0
$^2E\,-\frac{1}{2}\,u-$	0	$\sigma_{+\alpha}/\sqrt{6}$	$\sigma_{-\alpha}/\sqrt{3}$	$\pi_\alpha/\sqrt{2}$

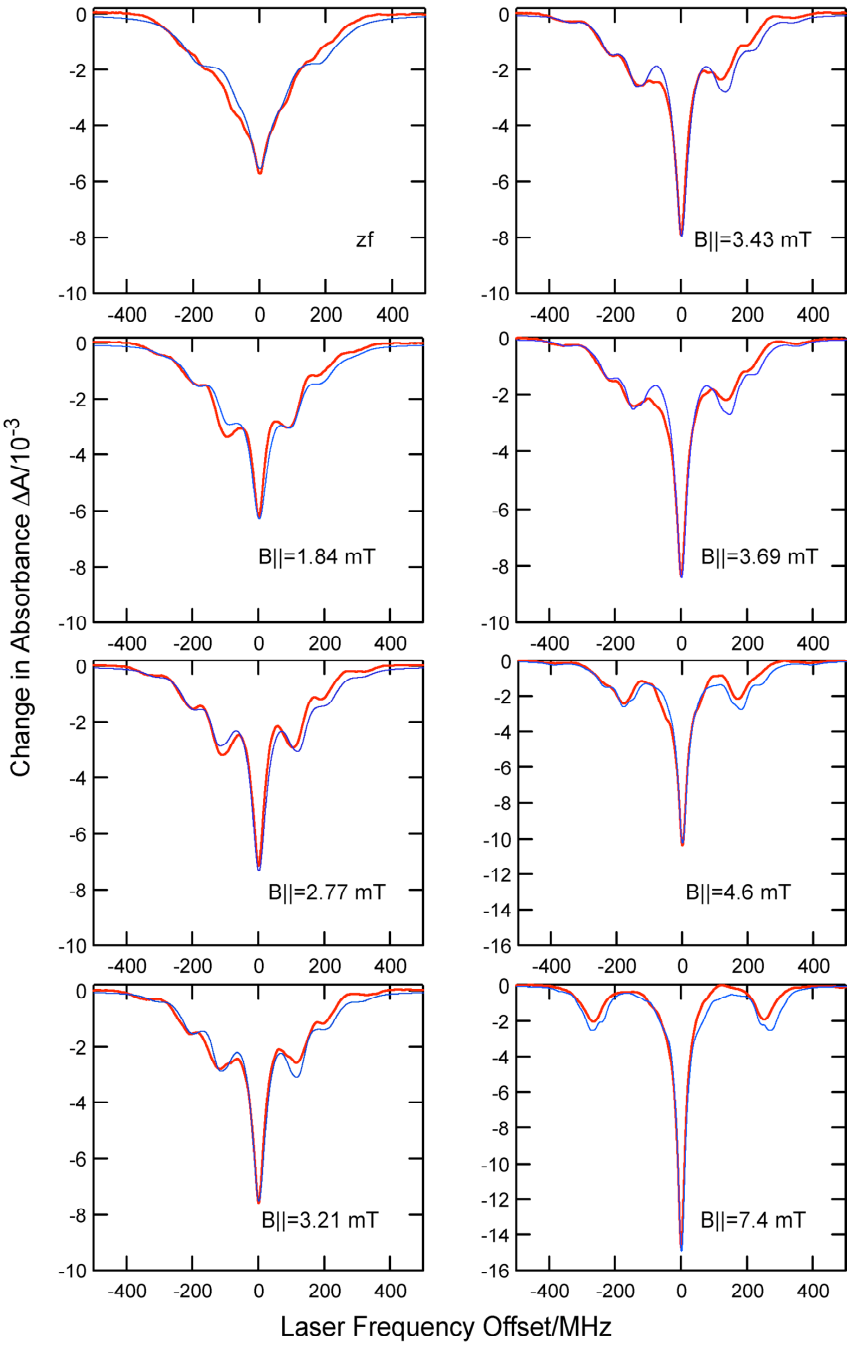

Fig. 3. Zeeman effect in the $R_1(\pm 1/2)$ line of 10 ppm $Al_2O_3:{}^{53}Cr$ at 3 K as observed in σ-polarized transient spectral hole-burning experiments in low magnetic fields of B||<7.5 mT. The red and blue line are observed and simulated (see text), respectively. The magnetic field flux B||c is indicated in the panels.

4. Conclusions

Hyperfine coupling in the ground and excited state leads to discrete sets of sideholes. Transient spectral hole-burning in low magnetic fields allows, in principle, the simultaneous determination of hyperfine coupling constants in the excited and ground states for transition metal ions in the solid state, given that the homogeneous hole width is narrow enough. The present report appears to be the first extensive investigation of hyperfine coupling in a transition metal ion by transient hole-burning. The value for A||($\overline{E}$ (^{2}E))=18 MHz in $Al_2O_3/^{53}Cr$ is commensurate with the value deduced form the digitized data displayed in Fig. 1. Geschwind *et al* showed that a quenched value of A|| in the $\overline{E}$ (^{2}E) state is expected as the orbital hyperfine field, to a certain extent, cancels the contribution by the core polarization field. The contribution by the orbital hyperfine field can be estimated by Eq. (5) [22].

$$H_{hf}^{orb} = 2\mu_B \left\langle 1/r^3 \right\rangle \Delta g \tag{5}$$

However, it appears that this cancellation in the $\overline{E}$ (^{2}E) level is less than originally reported [18] since the A|| value seems to be >6 MHz from the present experiments. The A⊥ value is close to the value of the spin-only $^4A_2$ ground state and the present evaluation appears to be the first attempt to measure this quantity in the title system.
We are presently in the process of conducting optical-rf double resonance hole-burning experiments in order to determine the hyperfine coupling constants in $Al_2O_3/^{53}Cr$ more accurately.

Acknowledgement

We thank the Australian Research Council for financial support of our research program. We are grateful to Hrand Djevahirdjian SA, Monthey, Switzerland, for providing us with boules of 10 ppm ^{53}Cr doped corundum.

References

[1] A.E. Becquerel, La Lumiere, ses causes et ses effets (Paris: Didot, 1867-1868)
[2] S. Sugano, Y. Tanabe, J. Phys. Soc. Jap. 13 (1958) 880.
[3] T.H. Maiman, Nature 187 (1960) 493.
[4] N. A. Kurnitt, I. D. Abella, S. R. Hartmann, Phys. Rev. Lett. 15 (1964) 567-568.
[5] A. Szabo, Phys. Rev. Lett. 27 (1971) 323–326.
[6] A. Szabo, Phys. Rev. B 11 (1975) 4512.
[7] P.E. Jessop, T. Muramoto, A. Szabo, Phys. Rev. B 21 (1980) 926.
[8] P.E. Jessop, A. Szabo, in Laser Spectroscopy V, ed. A. McKellar, T. Oka, B.P. Stoicheff, Springer-Verlag (1981) p. 408.
[9] P.E. Jessop, A. Szabo, Springer Series in Optical Sciences 30 (1981) 408.
[10] A. Szabo, J. Heber, Phys. Rev. A 29 (1984) 3452.
[11] A. Szabo, T. Muramoto, R. Kaarli, Opt. Lett. 13 (1988) 1075.
[12] A. Szabo, T. Muramoto, Phys. Rev. A 39 (1989) 3992.
[13] A. Szabo, T. Muramoto, R. Kaarli, Phys. Rev. B 42 (1990) 7769.
[14] A. Szabo, R. Kaarli, Phys. Rev. B. 44 (1991) 12307.
[15] A. Szabo, J. Lumin. 56 (1993) 47.
[16] (a) J. Ganem, Y.P. Wang, D. Boye, R.S. Meltzer, W.M. Yen, R.M. Macfarlane, Phys. Rev. Lett. 66 (1991) 695;
(b) J. Ganem, Y.P. Wang, D. Boye, R.S. Meltzer, W.M. Yen, R. Wannemacher, R.M. Macfarlane, Phys. Rev. Lett. 66 (1991) 1649.
[17] H. Riesen, B.F. Hayward, A. Szabo, J. Lumin. 127 (2007) 655.
[18] S. Geschwind, G.E. Devlin, R.L. Cohen, S.R. Chinn, Phys. Rev. 137 (1965) A 1087.
[19] V.V. Smartsev, A.M. Shegeda, A.V. Shkalikov, T.G. Mitofanova, Laser Phys. Lett. 5 (2008) 603.
[20] (a) A.A. Manekov, A.M. Prokhorov, Soviet. Phys. JETP 4 (1957) 288; (b) G.M. Zverev, A.M. Prokhorov, Soviet. Phys. JETP 7 (1958) 354.
[21] M. Naito, J. Phys. Soc. Japan 34 (1973) 1491.
[22] A. Abragam, M.H.L. Pryce, Proc. Roy. Soc. (London) A205 (1951) 135.